Proceedings of the ASME 2013 Summer Heat Transfer Conference
HT2013
July 14-19, 2013, Minneapolis, MN, USA

HT2013-17323

THERMODYNAMIC ANALYSIS OF ASPHALT SOLAR COLLECTOR (ASC)

Matthew Medas
University of Massachusetts Dartmouth
North Dartmouth, MA, USA

Rajib Mallick
Worcester Polytechnic Institute
Worcester, MA, USA

Sankha Bhowmick
University of Massachusetts Dartmouth
North Dartmouth, MA, USA

ABSTRACT

Hot mix asphalt (HMA) pavements are a potential source of extractable energy. Asphalt solar collectors (ASCs) have been designed and developed in the past as a means of extracting that energy. However, due to the variety of inefficiencies the potential for power generation has yet to be realized. This paper theoretically seeks to establish a better understanding of the performance and thermodynamic potential of the ASC. The ASC is compared to a solar water heater (SWH) through the use of (and modification to) the Hottel-Whillier-Bliss equation, a standard equation for the analysis of the SWH. Pipe spacing (W) plays a more significant role in affecting shape factor (S), Resistance Factor (F_{Res}) and and the thermal and overall efficiency of the ASC. It was established that minimizing pipe spacing or addition of a spreader layer (SN values in the range of 1-5) helped improve the thermal and overall efficiencies. The efficiency of ASCs would be in the 1-5% range, but the use of conductive spreaders can help increase it to 10%. Through this comparative analysis, several design changes can be suggested in key areas to optimize the ASC for the maximization of efficiency.

NOMENCLATURE

C_p	Fluid heat capacity
d_p	Pipe Diameter
D_p, D_{ins}	Pipe Depth
f	Fluid Friction Factor
F'	Collector Efficiency Factor
F_{ENT}	Entropy factor
F_{FR}	Friction factor
F_{HR}	Heat removal factor
F_{RES}	Resistance factor
G	Heat capacitance rate per unit area
h_{rad}	Radiation equivalent coefficient
h_s, h_p	Surface, Pipe Convection Coefficient
k_p, k_s	Pavement, Spreader thermal conductivity
L	Length of Pipe/pavement section
m	Fluid mass flow rate
q''_{losses}	Heat flux loss to environment
q_{in}	Incoming heat in pavement
q_s''	Incident Solar Flux
R_c, R_p, R_s, R_{net}	Pavement, Pipe, Surface, Net Resistance
Re	Reynolds number
S	Pavement Shape Factor
SN	Spreader number
T_f	Fluid Temperature
$T_{f,in}$	At inlet
$T_{f,out}$	At outlet
T_{INC}	Temperature ratio
T_p, T_s, T_{sky}, T_a	Pipe Wall, surface, sky, ambient Temperature
t_s	Spreader Layer Thickness
$\bar{V}$	Fluid average velocity
W	Pipe Spacing
α	Surface Absorptivity
ε	Surface Emissivity
$\eta_{overall}$, η_{th}, η_{carnot}	Overall, thermal, Carnot efficiency
η_{th}	Thermal Efficiency
ν	Fluid Viscosity
ρ	Surface Reflectivity

Copyright © 2013 by ASME

ρ_f Fluid Density

INTRODUCTION

Conventional solar water heaters typically have low efficiency and extract low-grade energy. ASCs represent an extreme case - having very low efficiency. Despite this, they still possess some merit due to the sheer amount of pre-existing road structure - the total amount of paved area in the United States is estimated to be around 39 million acres (157,900 km^2), 80% paved with asphalt pavement. Due to the nature of existing road structures (layers of aggregate and binder) and their perpetual need for maintenance (milling and re-paving due to damages like cracking and rutting), they can easily be converted to ASCs, providing for a plentiful source of low-grade energy. However, with various changes, the efficiency can be increased substantially, providing for more significant energy extraction. At the same time, the grade of energy that is being extracted can be increased, opening possibilities for alternative uses of the energy – such as operating a heat engine.

Dutch research group Ooms Avenhorn has done extensive work in the design, testing and development of the ASC, the Road Energy System™ (RES). Flowing water in embedded pipes cools and heats the pavement as necessary. Heat pumps are used in conjunction for climate control of nearby buildings [1]. Stresses around the piping were overcome through several design modifications [2, 3]. The piping was held in place by a rigid interlocking grid. A soft asphalt mixture was also used to prevent stress concentrations. A polymer-modified binder increased durability and stress response at temperature extrema, maintaining viscosity and deformation resistance with age [4]. The RES has been tested in a variety of regions, reducing temperature-related damages in high traffic areas and extracting heat in others [5]. Economic analyses have been done on the RES. The Dutch group determined that a 4,000 m^2 collector area would be sufficient in conjunction with a heat pump to reduce the fuel usage of a 10,000 m^2 building by 55%. [5]. Siebert and Zacharakis found that the ASC would pay for itself in terms of the energy benefit it provides and the savings in fuel, provided the materials did not cost too much [6]. The information published on the RES suggests that the average thermal efficiency is roughly 30%. No discussion on the grade of energy is given, although the temperature of the water was raised from about 8° to 14-18°C on average. The pavement surface temperature was reduced by about 3.5°C on average. Changes to soil temperature suggest that the storage system may spread heat underground [2].

The research group at Worcester Polytechnic Institute (WPI) has done a considerable amount of investigation into the performance of ASCs. Chen performed FEA and small- and medium-scale studies on the embedded heat exchanger [7]. The type of aggregate material was found to substantially affect conductivity. Adding copper and aluminum powder failed to increase conductivity, possibly due to surface oxidation or contact resistance. The conductivity of the pipe and its contact with the pavement strongly influence heat transfer [7]. Serpentine pipes did increase heat transfer, establishing the need for relatively close pipes. Dark glass (prevent surface loss) and surface coatings (decrease reflectivity) increased the outlet temperature. Carelli developed a tool to determine the economic viability of an ASC, showing that some locations within 30º lat. of the equator can be economically viable, despite the initial costs (predicted payback period of 7 or less years) [8, 9]. Structural analysis showed that the major stress concentrations are around the pipe, but at any depth, the stresses were far below the yield strength, even at a depth of 1"[8].

Hasebe et al. performed FE analysis of the ASC, utilizing a thermoelectric generator (TEG), but only a small amount of energy could be generated (estimated ~0.1 W/m^2)(no thermodynamic results) [10].

Material thermo-physical properties govern the behavior of the pavement and the ASC; mixture properties may vary locally. The poor thermal conductivity of asphalt impedes heat transfer. Luca and Mrawira estimated the conductivity of HMA to range from 0.74-2.89 W/m·K. Pavement surface properties are also important. The absorptivity of most asphaltic materials is estimated to be between 0.8 and 0.9 [11] and does not vary substantially with wavelength. Similarly, the short-wave emissivity of asphalt is typically about the same as its absorptivity, around 0.8 to 0.9 [11]. As the asphalt ages, these values may decrease moderately [11, 12].

Several studies have performed thermodynamic analyses on conventional solar water heaters (SWHs) to evaluate efficiency. Xiaowu and Ben performed one such analysis on a domestic scale collector. The estimated average thermal efficiency was 15.1% and the Carnot efficiency was 0.77%. They suggest that the most significant exergy losses occur from the storage tank, while altering the cover panels may increase the Carnot efficiency to up to 3.5% [13]. Kumar and Rosen evaluated the performance of an integrated collector-storage SWH utilizing a corrugated surface to increase heat transfer area. They estimated the thermal efficiency to be as high as 71%.Although no direct exergy analysis was performed, they reported that the maximum fluid temperature was roughly 64°C. (the Carnot efficiency could be as high as 14%, although generally much less) [14]. Al-madani estimated the maximum instantaneous thermal efficiency of a cylindrical SWH to be roughly 30-41% based on environmental conditions. No direct exergy analysis was performed. However, given a maximum temperature of 64°C and a maximum temperature difference of 27°C, the maximum Carnot efficiency can be estimated to be roughly 8% [15].

Solar ponds may achieve thermal efficiencies of up to 30%. However, they are expensive and many factors contribute to difficulty maintaining the proper conditions for adequate energy absorption [16].

An organic Rankine cycle or Kalina cycle is suitable for electricity generation given a heat source temperature of about 75°C or above [17]. As is true with all heat engines, the efficiency of this conversion increases with the temperature of the heat source. Solar concentrating collectors allow for a much

Copyright © 2013 by ASME

higher heat source temperature by reflecting sunlight off many mirrors onto a central absorber. Dish-type concentrators are designed as a single array of mirrors which moves to track the sunlight. Heliostat solar collectors use massive fields of reflectors which independently move to reflect the light onto a single collector tower. The thermal efficiency of heliostat collectors can reach as high as 98% [17]. Even if a solar water heater is unable to produce water at a temperature sufficient for power generation, the heated water can be used for process heat. Many chemical/industrial/manufacturing processes require a low-grade source of heat for completion. 30% of today's process heat applications use energy from 30-100°C; [17] this would be a suitable pairing with the ASC, particularly in the sense of utilizing the parking lots and roads surrounding an industrial complex (food and fabric processing, etc). In addition, the heated water available from the ASC can be used for a "pre-heating" stage in one of many power cycles, such as an Organic Rankine or Kalina cycle.

Photovoltaic (PV) cells are a much different technology than conventional SWHs, as they convert light more directly into electricity. Green *et al*. assembled a compendium of the efficiency of PV cells, describing a range of 6.4-41.1% efficiency [18].

OBJECTIVE

While the efficiency of ASC technology is much lower than that of PVs and conventional solar water heaters, the sheer amount of paved space that can be converted to ASCs is tremendous. The energy potential of ASCs has been evaluated and can be economically viable in certain areas. While conventional SWHs have been analyzed, the ASC is a relatively new topic and has not been analyzed thoroughly. This paper presents a basic theoretical thermodynamic/heat transfer analysis of the ASC in order to maximize the efficiency while minimizing the amount of changes to existing pavement design necessary. Various properties of the collector are combined into conjugate variables which are explored as a means of defining the performance characteristics of the ASC. Additionally, limiting factors in the design (key aspects limiting heat transfer) are identified as areas that require more development, and solutions suggested as a means of remedying such flaws. For example, a thermally conductive spreader layer (that would be placed in the same way as a geotextile layer) coupled to the pipes will increase the effective area of the pipes (allowing for higher efficiency with fewer pipes).

Table 1: material properties, dimensions and boundary conditions of the ASC

Description	Variable	Range
Incident Solar Flux	q_s''	300-1200 W/m^2
Surface Convection Coefficient	h_s	0-10 W/m^2·K
Surface Reflectivity	ρ	0.05-0.3
Surface Absorptivity	α	0.7-0.95
Surface Emissivity	ε	0.7-0.95
Ambient Temperature	Ta	5-30°C
Pavement thermal conductivity	k_p	0.5-2.5 W/m·K
Spreader Layer Thickness	t_s	0-15 mm
Spreader Layer Conductivity	k_s	20-1000 W/m·K
Pipe Spacing	W	0.1-2.0 m
Pipe Depth	D_p	0.025-0.1 m
Insulation Depth	D_{ins}	0.0-0.093 m

Several constraints (material properties, dimensions and boundary conditions) have been established for the initial design and analysis of the ASC. These constraints are listed in table 1.

MODELING AND ANALYSIS

Figure 1A depicts the arrangement of the ASC. A series of pipes of diameter d_p are embedded in parallel (repeating with a spacing of W between pipes) in the pavement (of conductivity k_p) at some depth D_p beneath the surface. The figure shows a symmetric half-section. The conductive spreader layer of thickness t_s and conductivity k_s is placed such that it lies horizontally between the pipes, assuming good contact between the two. Beneath the pipe and spreader layer is some intermediate amount of pavement material. At some depth D_{ins}, the lower boundary is considered insulated. This depth can be varied by placing a layer of insulating material.

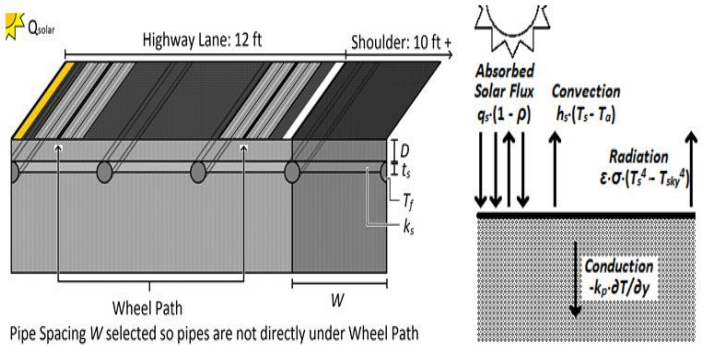

(A) **(B)**

Figure 1: A-Asphalt solar collector/heat exchanger and; B- energy balance at surface or pavement [24].

Table 2: heat transfer equations

Location and Mechanism	Governing Equation
Sub-domain (pavement, spreader) - Conduction	$k_y \cdot \partial^2 T/\partial y^2 + k_x \cdot \partial^2 T/\partial x^2 = 0$
Top Surface BC - Convection with ambient air	$q = h_s(T_s - T_a)$
Top Surface BC - Radiation to ambient objects	$q = \varepsilon \cdot \sigma(T_s^4 - T_a^4)$ σ- Stefan-Boltzmann const. $5.67 \cdot 10^{-8}$ J·m^{-2}·s^{-1}·K^{-4}
Top Surface BC - Absorbed Solar Flux	$q = q_s$
Pipe Wall BC - Convection	$q = h_p(T_p - T_f)$
All Other BCs - Insulated	$q = 0$

Figure 1B depicts the energy balance at the surface of the collector. The surface with reflectivity ρ is subject to

Copyright © 2013 by ASME

incident solar flux q_s. Energy is lost from the surface through convection (with coefficient h_s) and radiation (with surface emissivity ε) to the ambient (with temperature T_a). The energy that is not lost is absorbed and conducted down into the pavement. Table 2 lists the heat transfer equations applied for the boundaries and conduction (pavement and spreader) domain.

CONDUCTION RESISTANCE IN PAVEMENT COLLECTOR

Solar collectors utilize series of many closely-placed tubes. Conduction analysis is typically 1D due to the simple geometry. Our goal was to present a 2D problem in terms of a well-known 1D solution. In ASCs, a 2D analysis must be used, as the low conductivity of the pavement material and requisite depth of the pipes below the surface complicate the problem. However, this can be treated as a 1D problem by numerically determining the equivalent resistance to heat transfer. Since conduction is the only aspect of this problem which is 2D, only the conduction aspect was solved numerically. Although the 2D model could have been expanded to include surface effects, the comparison to the Hottel-Whillier-Bliss equation would be lost. Steady-state conduction through a multidimensional domain of constant conductivity k with two isothermal surfaces can be represented by an equivalent conduction shape factor S, using the Fourier equation:

$$q_{in} = -k \cdot A \cdot \frac{\partial T}{\partial x} \approx -k \cdot A \cdot \frac{\Delta T}{\Delta x} \approx S \cdot k \cdot \Delta T \quad (1)$$

The shape factor S was calculated through a series of steps, using finite element technique with COMSOL™ (general heat transfer module):

1. The geometry was created in COMSOL and assigned a constant thermal conductivity k_p.
2. Different temperature values were assigned to pipe wall and top surface (T_p and T_s); $\Delta T = T_s - T_p$
3. The steady-state heat transfer problem was then solved. Each model was meshed with triangle elements and a maximum element edge length of 0.0015m. The grid size corresponds with the dimensions of the model; i.e. W = 40 cm represents a grid size of roughly 160·100.
4. COMSOL's boundary integration feature was used to determine the amount of heat flux passing through the top surface. Conservation of energy was verified by comparing this value to the measured heat flux passing through the pipe wall.
5. Given the aforementioned measurements, the shape factor was calculated:

$$S = \frac{q}{k_p \cdot \Delta T} \quad (2)$$

6. The calculated values of S for each configuration were compared for a wide range of k_p and ΔT. S was a constant regardless of these values.

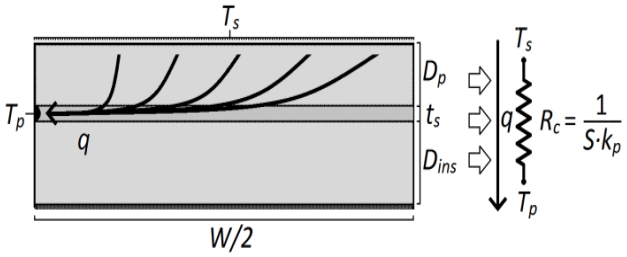

Figure 2: Conduction heat transfer schematic across the ASC.

Mesh independence was confirmed for each model (different mesh sizes due to change in geometry). COMSOL was configured to perform adaptive grid resizing, assuring mesh independence by re-iterating the problem with consecutively finer meshes until a converged solution invariant of mesh size was found.

The shape factor is a measurement of the mean conductive distance that heat must pass through from the top surface to the pipe, regardless of material properties. Once the shape factor was determined, the conduction resistance was calculated:

$$R_c = \frac{1}{S \cdot k_p} \quad (3)$$

Next, the conductive spreader layer was introduced as a means of improving heat transfer horizontally through the pavement [24]. The equivalent value of S was used to compare the improvement of adding the spreader layer. It was found that the conductivity and thickness of the spreader layer (k_s and t_s) have equal effect on the variation of S, and therefore their product SN defined as the Spreader No. was created:

$$SN = \frac{k_s \cdot t_s}{k_p} \qquad \textit{(Range from ~~1 to 5)} \quad (4)$$

Given the modification of the Hottel-Whillier-Bliss equation, conjugate variables were created, with the resulting thermal efficiency being represented:

$$\eta_{thermal} = F_{HR} \cdot (1 - e^{-F_{RES}}) \quad (5)$$

and the overall efficiency (product of thermal and Carnot):

$$\eta_{overall} = \eta_{thermal} - \frac{1}{F_{ENT} + \frac{T_{INC}}{(1 - e^{-F_{RES}}) \cdot F_{HR}}} - F_{FR} \quad (6)$$

Copyright © 2013 by ASME

(Derivations in appendix), where:

Resistance factor: The resistance factor represents the inverse of the net resistance of the ASC. In order to maximize heat transfer (and therefore maximize the utilization of the collected heat), the net resistance should be minimized. This, in turn, means that the resistance factor should be maximized. The flow rate should ideally be low such that the fluid undergoes some increase in temperature from inlet to outlet.

$$F_{RES} = \frac{F'}{G \cdot R_s} = \frac{L}{m \cdot C_p \left[\frac{R_s}{W} + \frac{R_c}{2} + \frac{R_p}{d_p \cdot \pi}\right]}$$

$$= \frac{L}{m \cdot C_p \left[\frac{1}{W \cdot (h_s + h_{rad})} + \frac{1}{2 \cdot S \cdot k_p} + \frac{1}{d_p \cdot \pi \cdot h_p}\right]} \quad (7)$$

Heat removal factor: The heat removal factor represents the fraction of heat incident at the surface that is not reflected or lost by other means. It accounts for the heat capacity and flow rate of the fluid in the collector piping as well as the surface area of the unit. The reasonable range for this variable is from 0 to 0.5.

$$F_{HR} = \frac{m \cdot C_p}{W \cdot L} \cdot \left(\alpha \cdot R_s - \frac{T_{f,in} - T_a}{q_s{}''}\right)$$

$$= \frac{m \cdot C_p}{W \cdot L} \cdot \left(\alpha \cdot \left[\frac{1}{h_s + h_{rad}}\right] - \frac{T_{f,in} - T_a}{q_s{}''}\right) \quad (8)$$

Entropy factor: This represents the total possible amount of entropy generated, assuming that all of the heat flow at the surface were brought to the temperature of the cold reference temperature. This also accounts for the flow and surface area of the collector. This parameter may range from 0 to 20.

$$F_{ENT} = \frac{q_s{}'' \cdot W \cdot L}{m \cdot C_p \cdot T_c} \quad (9)$$

Temperature ratio: This merely represents the ratio of the inlet fluid temperature compared to the temperature of the reference cold source used for the evaluation of energy grade (the cold reservoir temperature used for a heat engine). This may reasonably range from 0.8 to 1.2.

$$T_{INC} = \frac{T_{f,in}}{T_c} \quad (10)$$

RESULTS

1. Conduction shape factor for various designs

First, the shape factor S was calculated for the given ranges of pipe spacing W and pipe depth D_p. Figure 3 shows the results. The shape factor is largest when both W and D_p are the smallest. Both variables constitute the general length of the conduction path through the pavement. At wider pipe spacing, the shape factor is much less. Among the two parameters, W is dominant. Due to the dependence on W, it is clear that the pipes must be placed close together for optimum conduction.

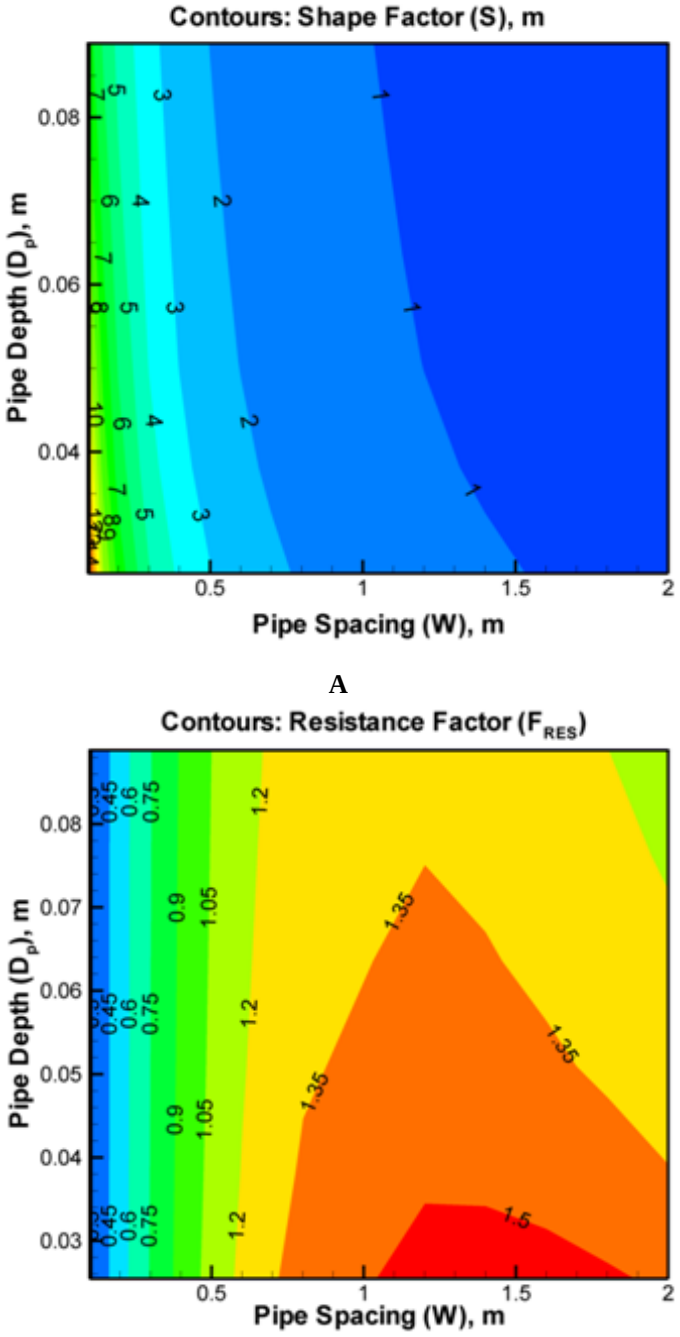

Figure 3: A- Conduction Shape Factor, comparing depth of pipe and spacing between adjacent pipes; B – resulting value of F_{RES}

Copyright © 2013 by ASME

Decreasing D_p will also enhance conduction, but will only have a significant effect if W is also small. The resistance factor is affected in a similar manner by D_p; the resistance factor is also decreased when the depth of the pipe is increased. However, increasing W increases F_{RES} due to its more substantial role in the calculation. Note the local maximum, showing how further increasing W begins to have less positive effects. This is due to the poor conduction over a long horizontal distance through the pavement to the pipe. In general, the pipe should be placed at a shallower depth if possible for optimum S and F_{RES}.

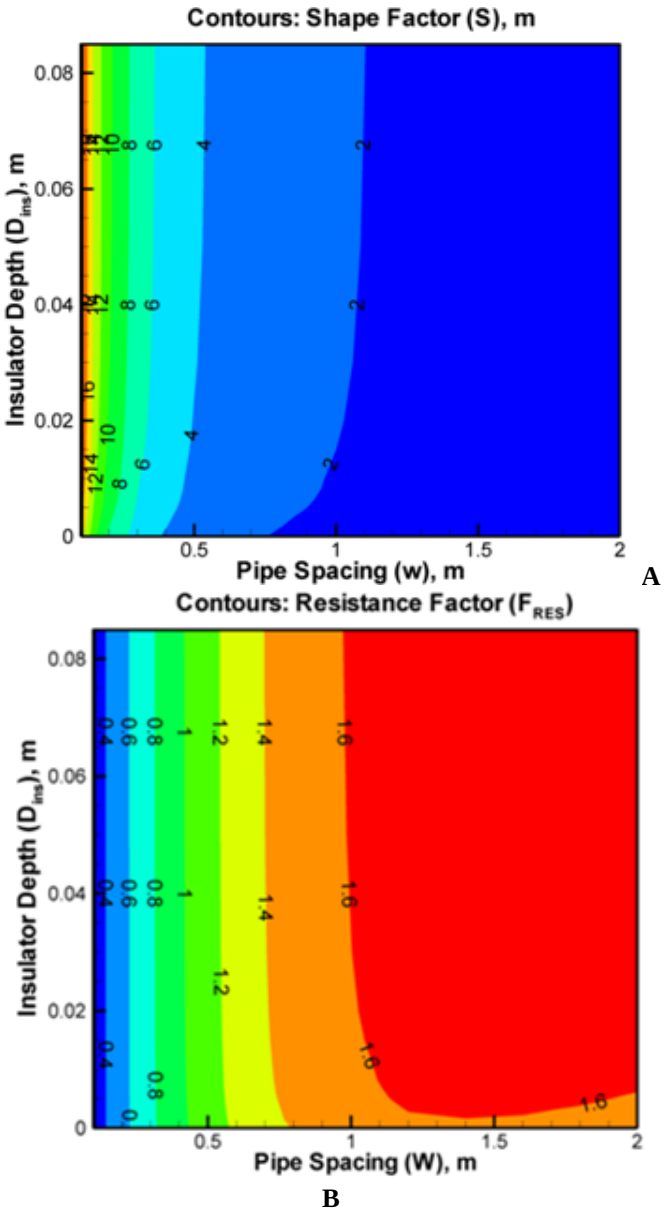

Figure 4: A - Conduction Shape Factor, comparing depth of insulator layer and pipe spacing, B – Resistance Factor

The pavement material underneath the pipes is important as it aids in conduction in the high-flux area around the pipe. Figure 4 shows the resulting value of S and F_{RES} through parametric variation of W and insulator layer depth D_{ins}. When an insulator layer is placed underneath the pipes at some shallow depth D_{ins}, it may partially restrict conduction into the pipe, and therefore reduce S. At larger W, the shape factor is not affected nearly as much, as the increased W hinders conduction substantially by itself. Similarly, the insulator layer depth has very little effect on F_{RES} which is again dominated by pipe spacing. The insulator layer does decrease F_{RES} slightly when it is placed closer to the surface, although its presence may significantly enhance the transient performance of the collector, as it limits the amount of material that can parasitically store energy that would otherwise be conducted into the pipes. (Not discussed in this paper).

Next, the equivalent value of S was calculated through variation of the SN and W. Figure 5 shows that by using a spreader layer with any reasonably high SN, S is dramatically increased. The spreader layer enhances horizontal conduction by providing a highly conductive channel for heat transfer towards the pipes. Also note that increasing the spreader number has a continuous significant effect at wider pipe spacing, showing how a spreader layer increases the effective area of the pipes. At small pipe spacing, the shape factor quickly reaches a plateau, whereas at larger pipe spacing, the shape factor continues to increase. The resistance factor is improved significantly with the addition of the spreader layer, particularly at wide pipe spacing. This is reflective of the spreader layer's role in improving conduction through the pavement, reducing the net resistance to heat transfer. The addition of the spreader layer shows the clearest improvement in both S and F_{RES} across the range of W.

In the calculation of the resistance factor, given the reasonable range of parameters (surface effects, conduction shape factor, pipe spacing, convection in the pipes), it was determined that the main limitations to heat transfer are due primarily to conduction, and to a lesser extent, to losses at the surface. Surface losses can be reduced by using a coating with solar-selective emissivity (materials such as black chrome [20], [21]) where the absorptivity of the surface will not be changed significantly but short-wave emissivity is significantly reduced. This will allow the surface to gain heat but give it off at a slower rate. From the results of this section, through variation of the given parameters, it is apparent that the resistance factor may range from roughly 1 to 3.5.

2. Efficiency

Given the results of the previous section, the thermal and overall efficiencies were calculated. Thermal efficiency was calculated as a function of F_{RES} and F_{HR} as shown in Figure 6. As expected, the thermal efficiency is proportionally related to the heat removal factor, agreeing with its definition – increasing the heat removal factor increases the amount of energy that is absorbed into the surface rather than lost to the

Copyright © 2013 by ASME

surroundings. The resistance factor is also proportionally related, as the net resistance of the collector should be minimized to maximize heat transfer. The resulting graph shows that a well-designed collector should optimize on both aspects for maximizing thermal efficiency.

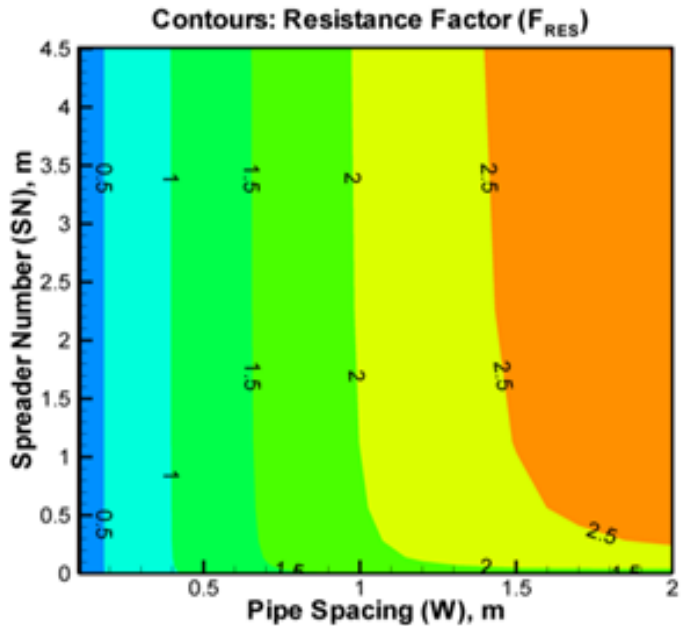

A

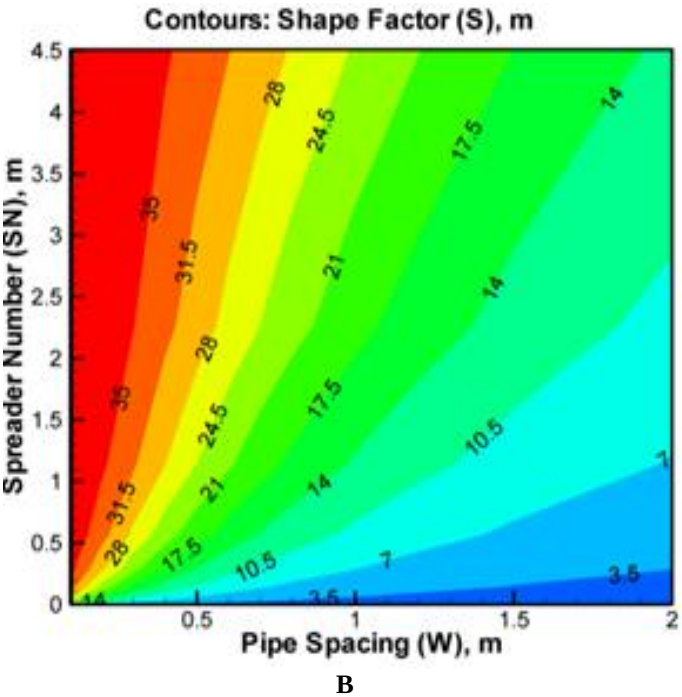

B

Figure 5: A- Conduction Shape factor, comparing pipe spacing and spreader number; B – resulting value of Resistance Factor

Next, the overall efficiency contours were plotted against the entropy factor F_{ENT} and the thermal efficiency (Figure 7). As expected, the thermal efficiency is proportionally related to the overall efficiency due to its role in the product. F_{ENT} is also proportionally related, as the grade of energy is inversely related to the temperature of the cold source used for the heat engine for energy conversion.

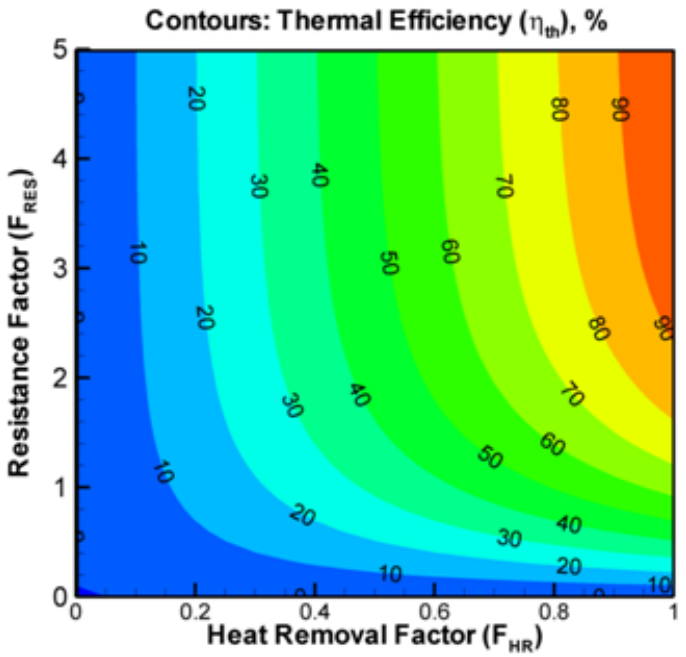

Figure 6: Thermal efficiency of ASC, comparing resistance factor F_{RES} and Heat Removal Factor F_{HR}

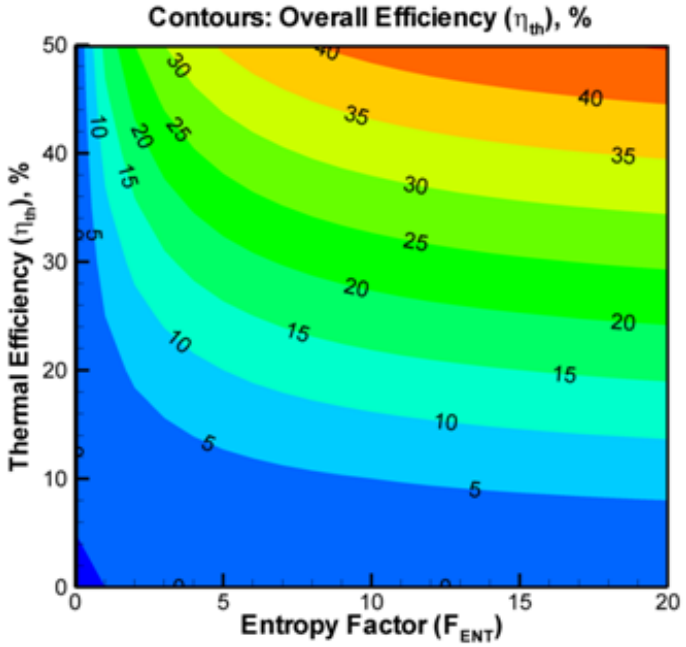

Figure 7: Overall Efficiency of ASC, comparing Thermal Efficiency η_{th} and entropy factor F_{ENT}

Finally, the overall efficiency was determined as a function of the thermal efficiency and temperature ratio. The temperature ratio is proportionally related to the overall

Copyright © 2013 by ASME

efficiency, again as the temperature of the cold source used for the heat engine for energy conversion. However, the temperature ratio plays a smaller role than expected, as the reasonable range for this variable is small and not enough to make a significant difference.

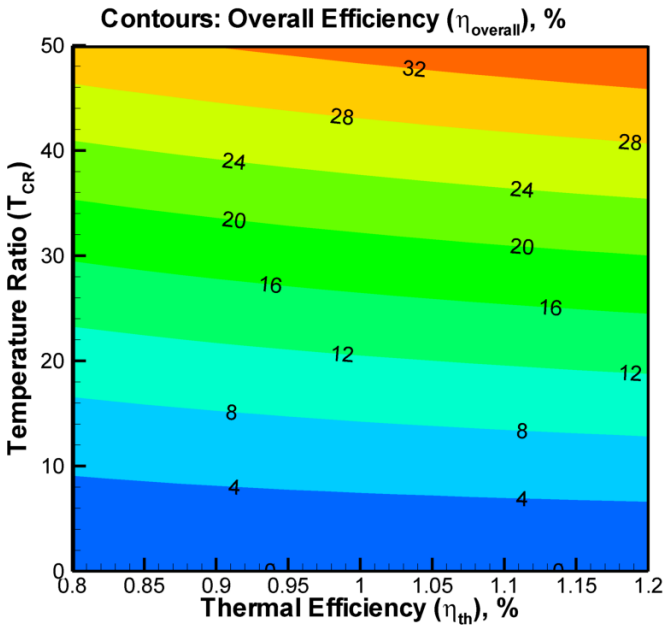

Figure 8: Overall efficiency of collector, comparing thermal efficiency and temperature ratio

DISCUSSION

The energy potential of HMA pavement is immense, given the tremendous amount of paved area in the world. The proposed means of utilizing this energy is through the use of the ASC, originally presented by the Dutch Group (RES). A heat exchanger embedded in the pavement will transfer energy to fluid in the pipes, which can be transported out for storage and use. Several different parameters may be varied to optimize the asphalt solar collector, maximizing efficiency while minimizing structural effects and additional costs. Conduction through the pavement has shown to be the biggest impediment. The main drawback of the ASC is based on the fact that HMA materials have poor thermal conductivity, which tends to inhibit heat transfer and limit the amount of energy which can theoretically be extracted for use. It is clear that the thermal conductivity of the pavement must be improved. The addition of conductive fillers may enhance the conductivity of the pavement (k_p) to aid heat transfer. Increasing the conductivity of the pavement material by such means has been investigated [22], [23] with mixed results. The poor conductivity of the pavement materials inhibits heat transfer not only in terms of the potential amount of extractable heat, but also requires that the pipes be placed very closely together, resulting in increased material costs and construction time, as well as structural and flow friction concerns from using so many pipes. Efficiency can be increased by placing the collector pipes at shallower depths (small D_p) or very closely together (small W), at the expense (structural and economic) of using a network of many pipes. The use of a highly conductive spreader layer to increase heat transfer to the pipes can be used to circumvent the problem. By using a conductive spreader layer of sufficient thickness (t_s) and conductivity (k_s) (forming some spreader number as defined previous SN), the net conductivity of the ASC unit can be increased without making a more significant modification to the HMA mixture, increasing efficiency and reducing in the number of pipes required to adequate design.

The heat transfer properties of the pavement surface may possibly be enhanced by using coatings to alter its solar absorption behavior. Materials such as black chrome [20], [21] have shown to have high general absorptivity (0.9) across the solar spectrum but have low emissivity (0.1) at temperature closer to 250F. This property, applied to the surface of the pavement, would effectively reduce the amount of energy lost to the environment while having little effect on absorption. This would increase the efficiency of extraction by limiting losses to the ambient.

The development of the asphalt solar collector as a means of effectively extracting energy for useful purposes is far from complete. This study has analyzed the performance of the collector at steady-state conditions. The high density and heat capacity of asphalt pavements requires more accurate transient conduction analysis. Once the transient performance has been explored, experiments should be performed to evaluate the validity of the steady-state and transient analyses. Potential issues, such as contact resistance and thermal expansion/contraction at the interface between the pipe and the pavement, must be investigated and eliminated or resolved as necessary. A suitable material for the conductive spreader layer must be selected, based on structural and economic analyses. Further experiments should investigate and evaluate the actual performance of the spreader layer. Finally, once the real-world performance of the collector has been fully evaluated, the optimum means of utilizing the extracted energy must be selected. Low-temperature utilization methods may include using the heated water as industrial process heat or as a pre-heating stage for some conventional power cycle. Provided the outlet temperature of the collector is 70ºC or higher, the proper fluid mixtures may be utilized for a Rankine or Kalina cycle [17].

Additionally, the structural integrity of the collector must be analyzed under different loads. Although piping has been used to reduce the temperature of pavements, mitigating heat-related damages due to the reduced stiffness, the ASC will not provide the same beneficial temperature reduction uniformly. In order to achieve adequate energy extraction, it is necessary that the fluid in the pipes absorb energy and increase in temperature as it passes through the ASC; the pavement surrounding the pipe at the outlet of the collector will still be very warm and susceptible to damages. These damages can be minimized by designing the ASC in several different sections based on their operating temperature and usage. The pavement regions at the inlet of the collector would be cooled the most,

Copyright © 2013 by ASME

and could therefore be used in a high-traffic area where loadings are the most severe. Intermediate areas with less frequent and less severe loadings, such as parking lots, could be used for fluid at an intermediate temperature. Areas of the collector where there are minimal loadings (areas such as sidewalks, etc) would feature fluid that is much hotter, as damages to the pavement will be much less likely. The Dutch group resolved these issues partially by using a softer asphalt mixture with a rigid grid to hold the pipes in place, as well as developing a polymer-modified binder to improve pavement stress response at a higher temperature range.

CONCLUSIONS

In the current study, a standard model for solar collectors, the Hottel-Whillier-Bliss equation, has been modified for more suitable application to asphalt solar collectors. The complex behavior of two-dimensional conduction throughout the asphalt pavement has been reduced using conduction shape factors to fit the one-dimensional treatment in the aforementioned equation. This adaptation includes delineation of the various physical parameters of the collector (pipe spacing, depth and insulator layer), as well as the inclusion of a highly conductive spreader layer for enhanced horizontal conduction. From this adaptation, a thermodynamic analysis of the ASC has been performed as a means of optimizing its performance and maximizing the thermal efficiency (amount of energy) and overall efficiency (amount and grade of energy).

We see that the performance of the collector is highly dependent on conduction occurring horizontally between the pipes. As such, the distance between pipes is a dominant factor. In addition, the conduction of the pavement material plays a significant role, as well as the addition of a highly conductive spreader layer.

ACKNOWLEDGEMENT

This work was funded by NSF CMMI 07030000.

REFERENCES

[1] Loomans, M.; Oversloot, H., de Bondt, A., Jansen, R. and van Rij, H., 2003, "Design Tool for the Thermal Energy Potential of Asphalt Pavements," Eighth National International Building Performance Simulation Association (IBPSA) Conference, Eindhoven, Netherlands.

[2] van Bijsterveld, W.T., Houben, L.J.M., Scarpas, A. and Molenaar, A. A. A., 2001, "Using Pavement as Solar Collector: Effect on Pavement Temperature and Structural Response," Transportation Research Record, Vol. 1778, pp. 140-148.

[3] van Bijsterveld, W.T. and de Bondt, A.H., 2002, "Structural Aspects of Pavement Heating and Cooling Systems," 3rd International Symposium on 3D Finite Element for Pavement Analysis, Design and Research, Amsterdam, The Netherlands.

[4] Srivastava, A., 2009, "Pavements: The Thermal Energy Potential of Asphalt and the Advantages of Polymer Modified Bitumen," Ooms Nederland.

[5] de Bondt, A. H. and Jansen, R., 2006, "Generation and Saving of Energy via Asphalt Pavement Surfaces," Ooms Nederland.

[6] Siebert, N. and Zacharakis, E., 2010, "Asphalt Collector and Borehole Storage - Design Study for a Small Residential Area," M.S. Thesis, Department of Energy and Environment (Building Services Engineering), Chalmers University of Technology, Goteborg, Sweden.

[7] Chen, B.-L., 2009, "Capture Solar Energy and Reduce Heat-Island Effect from Asphalt Pavement," Ph.D. Thesis, Civil Engineering Department, Worcester Polytechnic Institute, Worcester, MA.

[8] Carelli, J., 2010," Design and Analysis of an Embedded Pipe Network in Asphalt Pavements to Reduce the Urban Heat Island Effect," M.S. Thesis, Civil Engineering Department, Worcester Polytechnic Institute, Worcester, MA.

[9] Mallick, R.; Carelli, J., Albano, L., Bhowmick, S. and Veeraragavan, A., 2011, "Evaluation of the Potential of Harvesting Heat Energy from Asphalt Pavements," International Journal of Sustainable Engineering, Vol. 4, pp. 164-171.

[10] Hasebe, M.; Kamikawa, Y. and Meiarashi, S., 2006, “Thermoelectric Generators using Solar Thermal Energy in Heated Road Pavement,” 25th International Conference on Thermoelectrics, IEEE, Vienna, Austria.

[11] Luca, J. and Mrawira, D. M., 2005, "New Measurement of Thermal Properties of Superpave Asphalt Concrete," Journal of Materials in Civil Engineering, Vol. 17, pp. 72 - 79.

[12] National Cooperative Highway Research Program (NCHRP), 2004, "Mechanistic-Empirical Pavement Design Guide," Transportation Research Board, Washington, DC, Design Inputs.

[13] Xiaowu, W. and Ben, H., 2005, "Exergy Analysis of Domestic-scale Solar Water Heaters," Renewable and Sustainable Energy Reviews, Vol. 9, pp. 638-645.

[14] Kumar, R. and Rosen, M. A., 2010 "Thermal Performance of Integrated Collector Storage Solar Water Heater with Corrugated Absorber Surface," Applied Thermal Engineering, Vol. 30, pp. 1764-1768.

[15] Al-Madani, H., 2006, "The Performance of a Cylindrical Solar Water Heater," Renewable Energy, Vol. 31, pp. 1751-1763.

[16] Tabor H., 1980,"Non-convecting Solar Ponds" Philosophical Transactions of the Royal Society of London. Series A, Mathematical and Physical Sciences, Vol. 295 (1414), pp. 423-433.

Copyright © 2013 by ASME

[17] Goswami, Y. D., Kreith, F., and Kreider, J. F., 2000, "Principles of solar engineering," Taylor & Francis, 2nd edition, pp.314-315.

[18] Green, M. A., Emery, K., Hishikawa, Y. and Wilhelm W., 2009, "Solar Cell Efficiency Tables (Version 34)," Progress in Photovoltaics: Research and Applications, Vol. 17, pp. 320-326.

[19] COMSOL, 2008, "COMSOL Multiphysics User's Guide," COMSOL Multiphysics 3.5a.

[20] Hottel, H. C., and Whillier, W., 1955. "Evaluation of flat plate solar collector performance," Transportation Conference Use of Solar Energy Thermal Processes. Tuscon AZ.

[21] McDonald, G. E., 1975, "Spectral Reflectance Properties of Black Chrome for use as a Solar Selective Coating," Solar Energy, Vol. 17, pp. 119-122.

[22] Wu, S., Li, B., Wang, H., and Qiu, J., 2008 "Numerical Simulation of Temperature Distribution in Conductive Asphalt Solar Collector due to Pavement Material Parameters", Materials Science Forum, Vol. 575-578, pp. 1314-1319.

[23] Chen, M., Wu, S., Zhang, Y. and Wang, H., 2010, "Effects of Conductive Fillers on Temperature Distribution of Asphalt Pavements", Physica Scripta, (T139: 014046).

[24] Bhowmick, S., Medas, M., and Mallick, R., 2012, "Role of conductive spreader layer in reducing the surface temperature of HMA pavements," International Journal of Sustainable Engineering,Vol. 00, pp. 1-12

Copyright © 2013 by ASME

ANNEX A

EFFICIENCIES AND RESISTANCE FACTORS DERIVATIONS

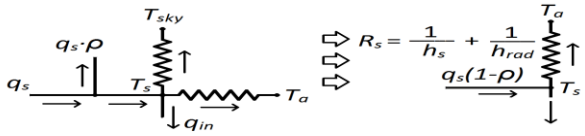

The thermal efficiency of a solar collector can be expressed through the Hottel-Whillier-Bliss equation (a standard equation for solar collector analysis):

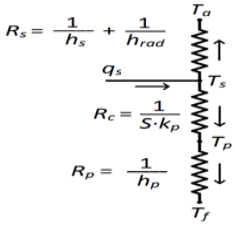

$$\eta_{thermal} = \frac{q_{extracted}}{q_{available}} = \frac{q_{in}}{q_s} = G \cdot R_s \left[1 - e^{\frac{-F\prime}{G \cdot R_s}}\right] \cdot \left[\alpha - \frac{T_{f,in} - T_a}{R_s \cdot q_s}\right]$$

$$G = \frac{m \cdot C_p}{W \cdot L} \qquad \theta = \alpha - \frac{T_{f,in} - T_a}{R_s \cdot q_s}$$

$$\eta_{thermal} = = G \cdot R_s \cdot \theta \left[1 - e^{\frac{-F\prime}{G \cdot R_s}}\right]$$

In this model, heat transfer is a series resistance problem. *F'* is the collector efficiency factor which represents the thermal resistance at the surface as a fraction of the net resistance. In order to use this equation, the individual resistances must be defined.

Surface Resistance

At the pavement surface, incident solar flux q_s'' reaches the surface, with a portion $q_s'' \cdot \rho$ reflected and the remaining $q_s'' \cdot (1 - \rho)$ absorbed. Heat is lost from the surface due to convection with the ambient air and outward radiation to the environment. Surface resistance R_s is defined such that it represents the total net loss at the surface, assuming heat transfer with the ambient:

$$q_{losses}'' \cdot W \cdot L = W \cdot L \cdot \frac{T_s - T_a}{R_s}$$
$$= h_s \cdot W \cdot L \cdot (T_s - T_a) + \varepsilon \cdot \sigma \cdot W \cdot L \cdot (T_s^4 - T_{sky}^4)$$

So, $$R_s = \frac{1}{h_s} + \frac{T_s - T_a}{\varepsilon \cdot \sigma \cdot (T_s^4 - T_{sky}^4)} = \frac{1}{h_s + h_{rad}}$$

Commonly accepted formula for solar panels:
$h_s = 5.7+3.8V$ (where V is wind speed in m/s)

Finally, the convection in the pipe has a resistance R_p, given coefficient h_p: $R_p = \frac{1}{h_p}$

Net Resistance/Efficiency Factor

Given the resistances, the net resistance R_{net} can be determined. *F'* is defined as the ratio of the surface resistance (losses) as a fraction of the total resistance to heat transfer:

$$R_{net} = \frac{R_s \cdot 2}{W} + R_c + \frac{R_p \cdot 2}{d_p \cdot \pi} \qquad F' = \frac{R_s \cdot 2}{R_{net} \cdot W}$$

Other intermediate resistances, such as contact resistance at the interface of the pipe/spreader and the asphalt, or resistance of the pipe material, may easily be added to this scheme.

The grade of the extracted energy is then evaluated, given the outlet temperature:

$$T_{f,out} = T_{f,in} + q_s'' \cdot R_s \cdot \theta \left[1 - e^{\frac{-F\prime}{G \cdot R_s}}\right]$$

$$\eta_{carnot} = 1 - \frac{T_c}{T_h} = 1 - \frac{T_c}{T_{f,out}}$$

$$\eta_{carnot} = 1 - \frac{T_c}{T_{f,in} + q_s'' \cdot R_s \cdot \theta \left[1 - e^{\frac{-F\prime}{G \cdot R_s}}\right]}$$

The overall efficiency is the product of the thermal efficiency and energy grade:

$$\eta_{overall} = \eta_{th} - \frac{T_c}{\frac{T_{f,in}}{\eta_{th}} + \frac{q_s''}{G}}$$

The Hottel-Whillier-Bliss equation for efficiency does not account for the energy lost through friction in the pipes. Particularly due to the low efficiency and tremendous amount of area required for the ASC, friction losses in the pipes must be included. Energy loss through pumping fluid has resulting effect on efficiency

$$\Delta Q = \bar{V} \cdot \Delta P \qquad \Delta\eta = \frac{-\bar{V} \Delta P}{q_s'' \cdot W \cdot L}$$

Darcy-Weisbach equation: $\Delta P = \frac{f \cdot L \cdot \rho \cdot V^2}{2 \cdot d_p}$

$$f = \frac{64}{Re} \qquad m = \bar{V} \cdot \rho$$

The overall efficiency including pipe losses is then:

$$\eta_{overall} = \eta_{th} - \frac{T_c}{\frac{T_{f,in}}{\eta_{th}} + \frac{q_s''}{G}} - \frac{128 \cdot \nu \cdot G^2 \cdot L^2 \cdot W}{\pi \cdot \rho \cdot C_p^2 \cdot d_p^2 \cdot q_s''}$$

Copyright © 2013 by ASME

This can be simplified by combining variables:

$$\eta_{overall} = F_{HR} \cdot (1 - e^{-F_{RES}}) - \frac{1}{F_{ENT} + \frac{T_{INC}}{(1 - e^{-F_{RES}}) \cdot F_{HR}}} - F_{FR}$$

Heat removal factor:

$$F_{HR} = \frac{m \cdot C_p}{W \cdot L} \cdot \left(\alpha \cdot R_s - \frac{T_{f,in} - T_a}{q_s{}''}\right) = \frac{m \cdot C_p}{W \cdot L} \cdot \left(\alpha \cdot \left[\frac{1}{h_s + h_{rad}}\right] - \frac{T_{f,in} - T_a}{q_s{}''}\right)$$

Resistance factor: $F_{RES} = \frac{F\prime}{G \cdot R_s} = \frac{L}{m \cdot C_p \cdot \left(\frac{1}{W \cdot (h_s + h_{rad})} + \frac{1}{2 \cdot S \cdot k_p} + \frac{1}{d_p \cdot h_p \cdot \pi}\right)}$

Entropy factor: $F_{ENT} = \frac{q_s{}'' \cdot W \cdot L}{m \cdot C_p \cdot T_c}$

Temperature Ratio: $T_{INC} = \frac{T_{f,in}}{T_c}$

Friction factor: $F_{FR} = \frac{128 \cdot \nu \cdot m^2}{W \cdot \pi \cdot \rho \cdot d_p^4 \cdot q_s{}''}$

$$\eta_{thermal} = F_{HR} \cdot (1 - e^{-F_{RES}})$$

Copyright © 2013 by ASME